

Mechanical Hip Prosthetic

Engineering Calculations Summary

Aiden Camisa, Project Manager | CAD Lead
Quinn O'Neill, Website Designer | Machinist
Matt Martinez, Fundraising Lead | Anatomical & ANSYS Lead
Victoria Lyon, Budget Liaison | Anatomical Lead

Fall 2025-Spring 2026



Project Sponsor: NextStep Prosthetics
Faculty Advisor & Sponsor Mentor: Dr. Dante Archangeli, Dr. Reza Razavian
Instructor: Professor David Willy

Top Level Design Summary

Hip disarticulations and hemipelvectomies are rare: accounting for only 1% percent of all amputees. Individuals subjected to these amputations are left to very limited solutions for mobility further than a wheelchair or crutches. The scope of this project is to design and fabricate an active hip prosthetic to address mobility discrepancies offered in the current market. This system is designed to fully support a 90 kg individual during walking, sitting and standing, and stair ascent/decent. The design will follow a natural range of motion within the sagittal plane and compatibility with all standard types of prosthetic knees and sockets.

The current model is composed of 2 sub-systems, including mechanical and electrical. A model of the design is detailed below, noting that majority of the electronics will be separately mounted:

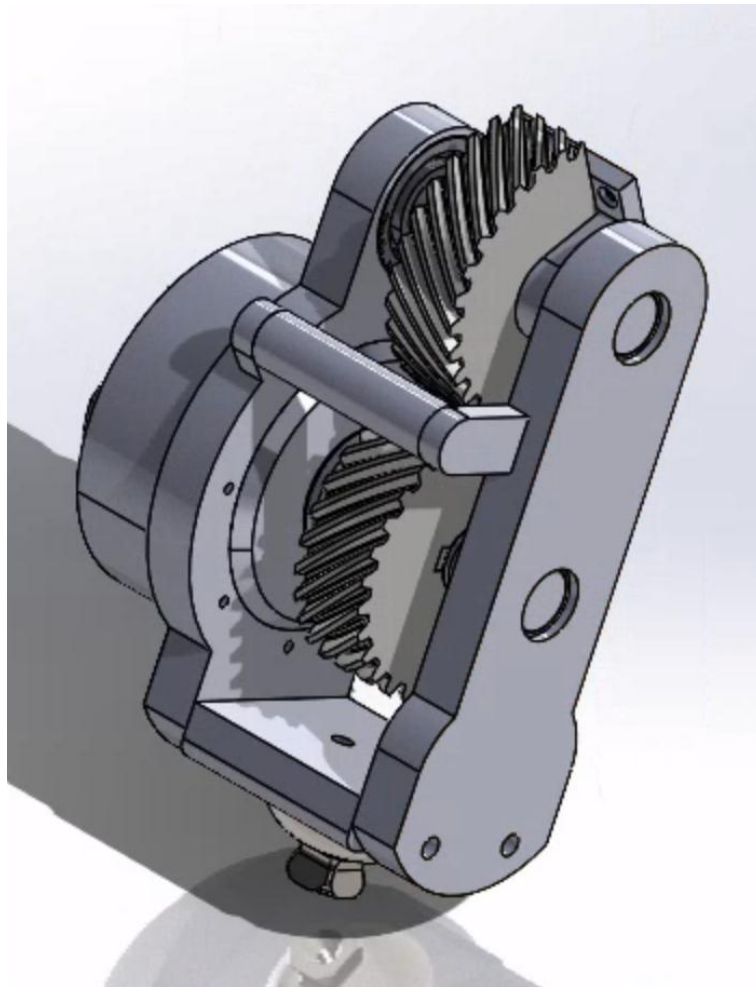


Figure 1:

To address both engineering and customer requirements, a QFD is utilized:



Figure 1: Quality Function Deployment

Our customer is a hip disarticulation patient who seeks to live a more active lifestyle than what is readily available to them with an unpowered hip prosthetic. These requirements include a stable leg, the ability to walk and climb stairs, easy and comfortable use, a non-cumbersome design, efficient battery life, and adaptable use. The stable leg implies the leg will be able to hold the weight of a 90kg user in standing and during all stages of the walking gait.

With each customer requirement stated, we turn each of these goals into quantifiable goals, or at the very least, better define them within the scope of our project. To make the leg stable to stand and walk on, it will need to be able to regularly withstand the reaction force of walking and the stress that causes. We calculated the maximum stress to be around 64.854 MPa during the walking phase. Our goal for an easy, non-cumbersome design will be defined with a weight that is less than 20lbs and a sleek, intuitive design that does not inhibit any comfortability or movement. For the range of motion, we determine that the hip joint should replicate a sound hip flexion and extension as closely as possible. This is quantified at about -20° in extension to 110° in flexion, with the assumption that 0° degrees is standing up straight. For the requirements of our motor, we need it to be able to lift the leg to around 110° from standing. The determined minimum torque for this motor will need to be 22Nm, assuming a gear ratio of 1 is used to transmit that torque to the leg.

Standards, Codes, & Regulations

- Motor standards

Our motor the Cube mars AK80-64 KV80 follows Ce and RoHS Standards promoting general safety of the device. It is Quality assured under the AS9100D and ISO 17804 standards assuring that it works as intended and promoted. It is rated under Class H insulation, allowing it to withstand up to 180 degrees Celsius. And it uses standardized communication protocols like CAN and UART

- Screws

All of the systems screw use mostly ISO metric standards or UTS standards. Both detail safety requirements but differ in forms of units used for standardization.

- Gears

Our gears are to be ordered from Boston Gears, which follow ASME and AGMA standards, abiding by standardized sizes for ease of use and safety thresholds.

- Bearings

Our Bearings Use ISO standards detailing international safety standards ensuring strong manufacturing quality and ABMA standards for standardized bearing sizes and bearing types

- Bracketing/Shafts

Our aluminums and steels follow ASTM international standards for metal strength and safety, ensuring our materials are of ample quality. The metals will be Machined in the NAU machine shop, which follos OSHA standards of safety and EPA environmental safety standards, along with additional codes specific to the shop.

- Battery

Our battery the HB Power Li-ion 10S1P2200AA01 uses a variety of different standards. It follows OSHA safety standards ensuring safety to those using the battery. It follows ROHS restriction of hazardous substance standards for not using overly dangerous materials. ISO standards for international safety codes. IEC standards for lithium safety. ANSI C18 standards for safety and performance requirements for specifically portable rechargeable batteries.

- Control Systems

Our control system uses a Raspi 5 and an Adafruit Feather. Both follow the safety standards of ESD electronics safety standards and IoT cybersecurity standards. They both use sizing standards of GPIO pins and I2C, SPI, and UART control standards. The wires use SWG wire gauge standards and ISO international safety standards. Any other standards for the control system are set by the standards of the batter powering it.

- IRB

The Institutional Review Board dictates standards and rules for testing a device like our prosthetic. The group will be completing the readings and trainings and has submitted the device to the IRB so we are ready to test our device in the safest way possible.

- Prosthetic devices

Our device will be designed to follow the safety codes set out by the Healthcare Common Procedure Coding System (HCPCS). The HCPCS sets codes depending on the area of amputation, in our case we follow the codes for L5250 through L5270.

Equations & Solutions

Majority of the load cases were analyzed at maximum point in the gait cycle where the hip joint experiences the most load, torque, and moment (of a 90kg individual). It is critical that the design is able to deliver structural stability and necessary power for the most load-intensive activity points on the hip joint. structurally able to handle normal activity. Each analysis specifies cases and scenarios used for calculations.

Forces on Leg Due to Walking – Quinn O’Neill

This analysis provides critical insights into the peak loads experienced by the leg during normal walking.

Reaction force is approximately 1.5 times body weight during heel strike/toe-off, and body weight at mid-stance for a 90 kg mass. – Foot length: 24.16 cm, shank length: 39 cm, foot at 90° to shank, heel/toes at 20° to ground. Reaction forces are modeled by:

$$R_1 = 1.5mg \quad (1)$$

$$R_2 = mg \quad (2)$$

R1 is the reaction force during heel strike and toe-off (N), R2 is the reaction force at mid-stance (N), m is the mass of the individual (kg), and g is gravitational acceleration (9.81 m/s²). A static equilibrium analysis is then performed to determine force and moment distributions and a geometric modeling of leg segments during gait phases (heel strike, mid-stance, toe-off):

$$\sum F = 0 \quad (3)$$

$$\sum Mk = 0 \quad (4)$$

where $\sum F$ is the sum of forces (N) and $\sum Mk$ is the sum of moments about the knee (Nm).

$$Ft = Fk \sin \theta \quad (5)$$

$$Fa = Fk \cos \theta \quad (6)$$

Ft is the transverse force (N), Fa is the axial force (N), Fk is the force at the knee (N), and θ is the angle of the force (degrees). - Maximum force: 1.324 kN during heel strike and toe-off

The maximum force of 1.324 kN and moment of 176.65 kNm highlight the need for robust materials and designs capable of withstanding these dynamic loads.

These calculations give us the preliminary reaction forces on the leg and will not need to be changed as they do not affect the design

Actuation Static Force Analysis – Quinn O’Neill

This analysis determines the force needed for actuators to achieve a 100° hip motion range by using moment and force balances for selecting actuators (hydraulic, pneumatic, and electronic linear). The equations that model this are equations (3) and (4) Center of mass (COM) percentages are 43% for the thigh, 43% the shank, and 42% for the foot. The results yield a required actuator force of 142.8 N for a 42.854 Nm moment.

The 142.8 N requirement allows selection from various actuator types, with cost as a deciding factor. All three actuator types (hydraulic, pneumatic, electronic) are viable, but the cheapest reliable option should be chosen for cost-effective design without compromising performance.

As we are still basing our general leg geometry off of that of a human leg, these calculations will not need to be changed.

Battery Analysis – Quinn O’Neill

The team needs a battery to power the motor to lift the leg. This battery must be chosen based on if it allows the motor to produce enough power, and the energy stored by the battery is enough to allow the user to use the leg for long enough.

To start, we need to find the required voltage of the motor. To do this we found the required torque and rotational speed of the motor based on a study and dataset detailing the amount of torque at the hip for lifting the leg, and the rotational speed at which it is lifted. Using the formula:

$$P = T\omega \quad (7)$$

Where P is power (Watts) T is torque (Nm) and ω is rotation speed (rad/s). Plugging the data and formula into MATLAB we got a graph that looks like this:

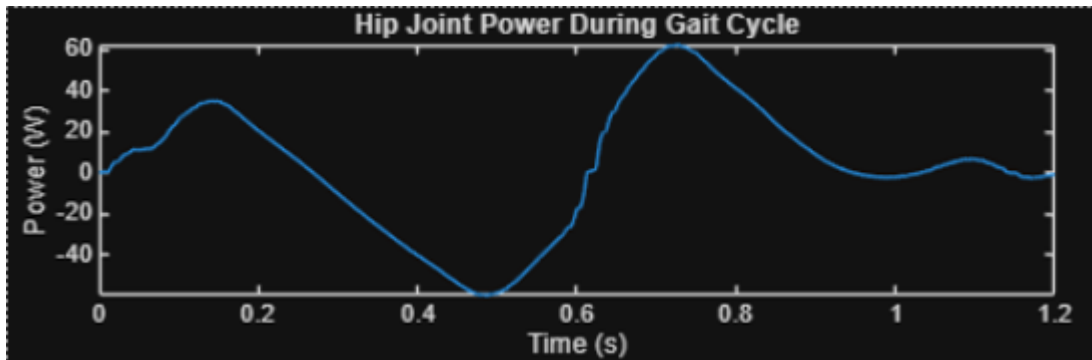


Figure 2: Hip joint power per gait time

From this data we get an average of 23.98 Watts per step. Then using listed data from our selected motor, the Cubemars AK8064 KV 80, we were able to find the required amperage per the gait cycle using this formula:

$$I = T/kt \quad (8)$$

Where I is current (Amps), T is torque (Nm), kt is a rated torque constant (Nm/A). resulting in following:

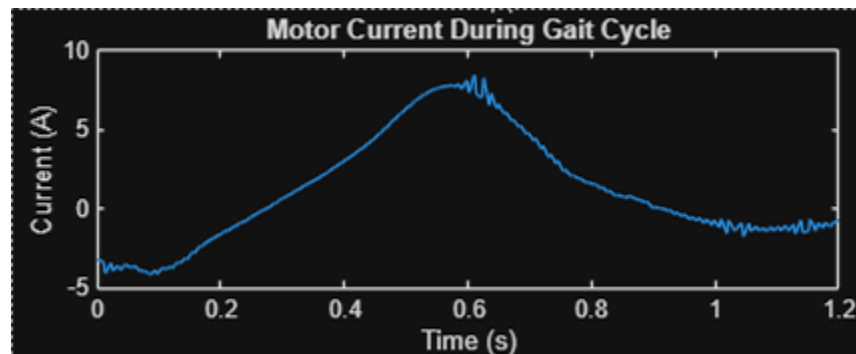


Figure 3: Motor current per gait time

Then doing a matrix division of the Power and the current results in the following graph, showing the voltage for the motor required.

$$V = P/I \quad (9)$$

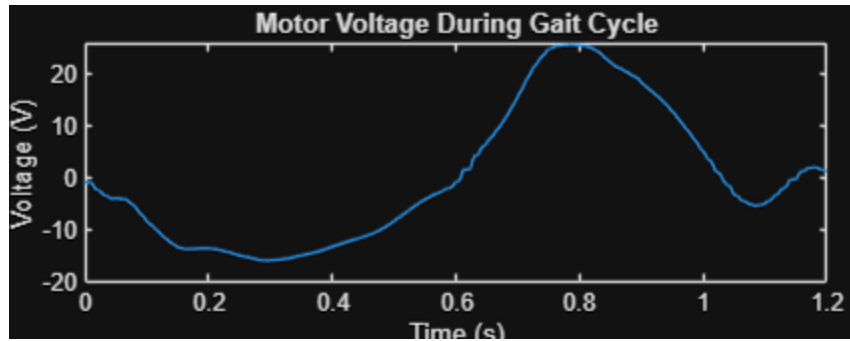


Figure 4: Motor Voltage per gait time

This graph gave us the Maximum motor voltage value of 25.7503 Volts. The motor is rated for Voltages of 12/24/36/48, meaning the minimum required input voltage for this to motor to function at its max efficiency is 36V.

Our next goal is to find how much energy we need for the users of our product to achieve what they want to and then find a battery with that Energy. First, we need to set a limit to our user's goal. We decided we wanted to allow our customers the recommended 10,000 steps a day for general fitness. Because we are only designing for 1 leg, we need to allow only 5000 per that leg, however since we want to allow our user to go above and beyond, and account for activity other than walking, we landed on an allowed 10,000 steps for our leg.

Taking the average power per step of 23.98 Watts and taking an average step time of 1.2s from our walking study, we can determine the Energy used per step with the following formula:

$$E = P * t \quad (10)$$

Where E is energy (Joules) and t is time (seconds), resulting in a step energy of 28.78 J. Multiplying by our desired step count of 10,000 we get a required energy of 287,800 Joules stored within the battery. Most batteries have a listed number of Amp-hours or Watt-hours. Watt hours are a form of energy stored in a battery per full charge. Amp-hours can easily be converted to Watt-hours by multiplying our chosen battery voltage. Converting our Energy to Watt hours resulting in a required battery rating of 79.9 Wh or 2.22 Ah.

This formula allowed the team to choose the battery we are using. That battery is able to power our motor reliably, and because we haven't changed our motor these calculations are still up to date.

Static Force Frame Analysis – Aiden Camisa

Introduction

The hip prosthetic uses many systems including; electric motors, gear systems, and the frame that supports the system. To ensure the safety of structural reliability, critical frame components must be analyzed to verify that they can withstand the mechanical loads experienced during daily activities.

The lower limb attachment structure plays a significant role in transmitting ground reaction forces into the prosthetic hip system. The original design incorporated two curved side brackets; however, after additional research and discussion with the client, we decided to look at a possible redesign of a single straight bar across the interior of the frame. This reduces space within the center of the design, improves

manufacturability, and reduces the weight and length of the device. To evaluate this new design vs the old one, I performed a numerical comparison on the yield stress of this new design compared to the old design and a factor of safety (FOS) calculation for the edges around the side mounting brackets. Finally, to tie it all in, I did a Finite Element Analysis (FEA) within solid works, to see the visual comparison of these two designs. Using these three contributing factors we are able to make a informed and final decision on our design.

Assumptions

Below are the assumptions I used for the calculations and the analysis. They each will have a justification as to the assumption that is used and why those values were chosen. They are then broken down into sections so that it is clear where and when I used these values.

Material Properties

For the material for the frame, we have looked at using Aluminum 6061-T6. We chose this because it is lightweight, widely used within prosthetic frame designs, and its ease of machinability.

Load Assumptions

When looking at the load of the prosthetic goal, we use the estimation 90kg individual as this is within our customer requirements. We then use this to multiply by gravity to get a value for the body weight of 883 N. This is then divided by 2 to get the load for each user's legs. Another force we accounted for is the force of the step on the ground. This gets a reacting force from the lower leg of 1324 N. Finally, we have the torque from the motor that we use on the rest of the leg. This value is 48 N*m for the continuous torque or 120 N*m for the Peak torque during short duration movements. For the analysis in this paper, we take the worst case of the short duration movements for the calculations.

Schematics

Within this there are multiple parts that make up the design. In Figure 1, we can see our current entire design. On each end is the side mounting brackets that hold the motor and the bearings in place. Connected to them is the current design of the lower attachment bracket. The side brackets are used to hold everything in the axial direction whereas the lower holds each piece together and connects to the lower leg by use of a female pyramid adapter which is a industry standard within knee prosthetics.

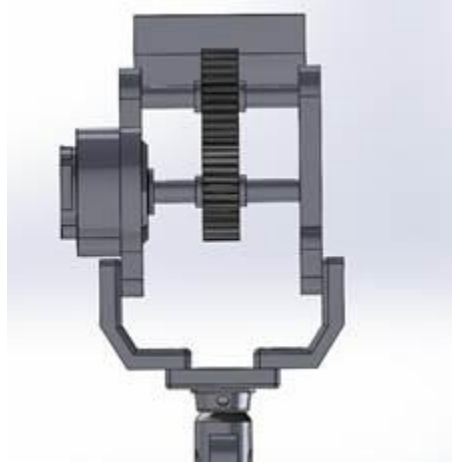


Figure 5: Current Prosthetic Design

Here we can see the design above. In initial designs, it was left larger as it would leave space for electric systems. However, as we made more decisions about the system, we determined that it would be better to create as small and strong of a system as possible to decrease weight and allow for it to fit more users.

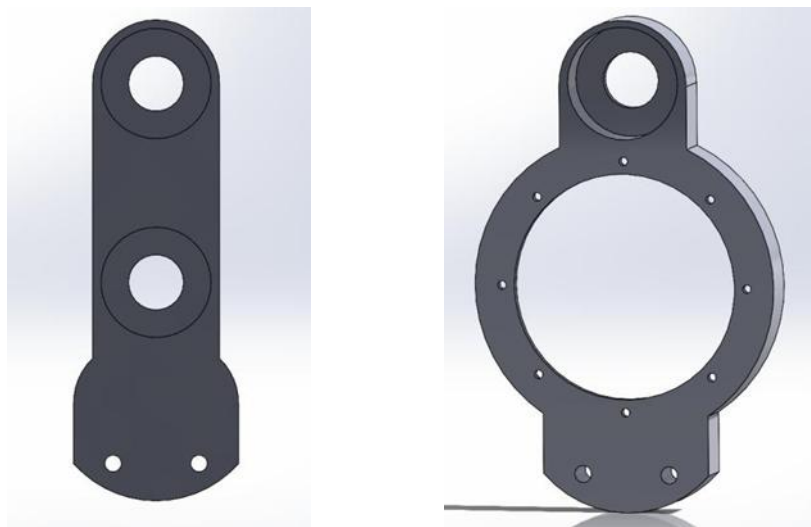


Figure 6: Non – Motor Side bracket Figure 7: Motor Side Mounted Bracket

In the images above, in figures 6 and 7 we see the side mounted brackets. While similar in dimensions, there are some differences between the two. Both brackets are 15 mm thick and 60 mm wide and 175 mm long. Each bracket has a 40mm diameter hole that it sits in, with a thickness of 6.11 mm. Each hole that connects to the lower bracket is a 6 mm hole.

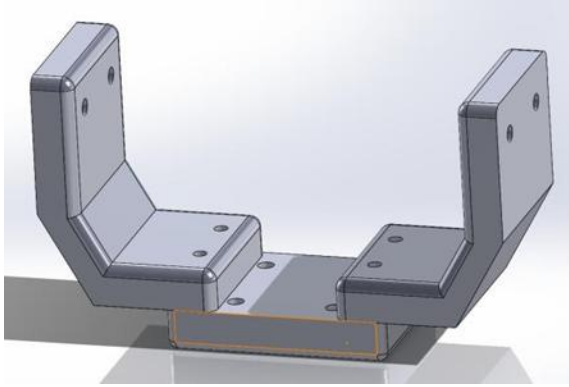


Figure 8: Current lower bracket

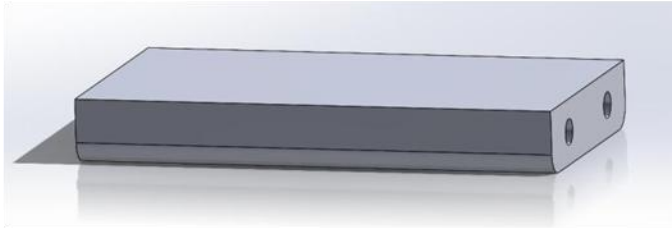


Figure 9: New lower bracket

Above in figures 8 and 9 we have lower attachment designs. The current design works around side mounted frames however the new bracket goes between the two mounts. For the current design is broken into 3 parts. With two slightly “L” shaped brackets and a straight lower bracket that connects to each “L”. In the new design the lower bracket acts as a bridge between the two side mounted brackets. The dimensions for this are 60mm wide, 15mm thick, and 111 mm long, with two holes in each side for screws to go through allowing for easy installation.

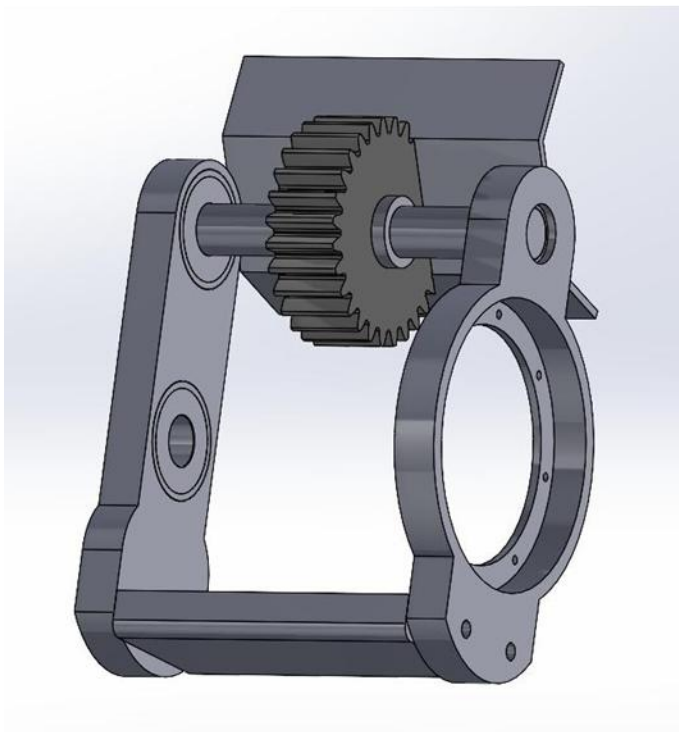


Figure 10: New Frame design Model

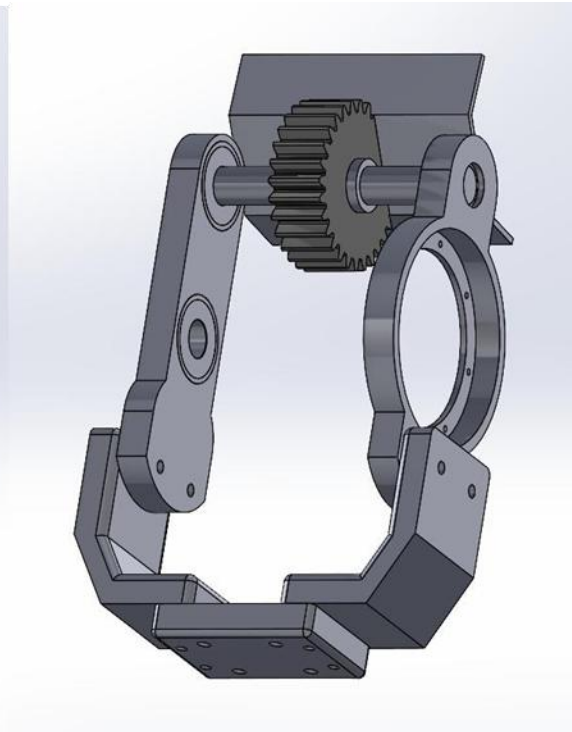


Figure 11: Current Frame design Model

Above is the full design of each frame with the motor and the lower shaft being removed. These are also used for the FEM analysis and below you can see the mesh systems of these solid work modes.

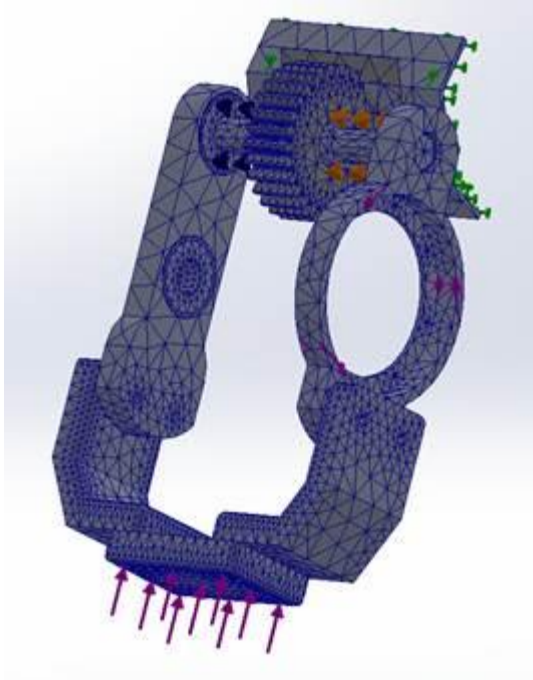


Figure 12: Mesh of Current Frame design Model

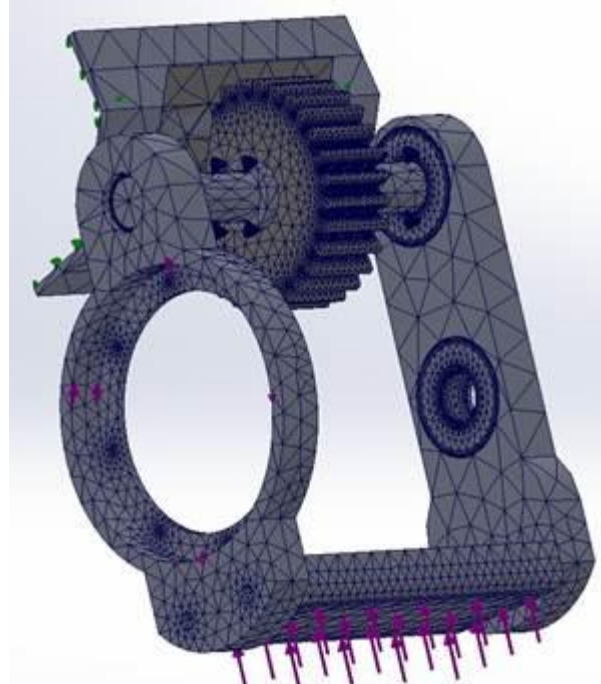


Figure 13: Mesh of New Frame design model

Equations Used

With the assumptions and schematics of each of the parts listed above, we can use the equations listed below to calculate and determine the yield stresses and the FOS for the thickness around the bearings. In addition, I will also describe the Analysis settings that were used in the FEMA for these calculations. This aluminum does have a yield strength of $\sigma = 276$ MPa. We also decided to enforce a minimum FOS for are yield of 2. This means that the σ allowable is 138 MPa. For force calculations, I determined the net force and used this in the system by evaluating using the reaction force and the body weight force to get a $F_{net} = 441$ N.

$$M_{Bending} = F * L \quad (11)$$

Equation 11: Bending moment due to a central load being applied, in Newtons

$$I = \frac{b * t^3}{12} \quad (12)$$

Equation 12: Moment of Area, in m^4

$$I_{ring} = \frac{\pi(D_0^4 - D_1^4)}{32D_0} \quad (13)$$

Equation 13: Moment of Area for hollow ring

$$\sigma = \frac{M_{Bending}}{I} \quad (14)$$

Equation 14: Stress equation, MPa

$$FOS = \frac{\sigma_{yield}}{\sigma} \quad (15)$$

Equation 15: Factor of Safety for current vs. new design.

Using these equations, we are able to calculate both the FOS for the new design compared to the old design and the possible yield stress around the thin parts of the bearing frame. In addition to this I use these consistent settings for the finite element method analysis. For the material of the part I use the aluminum 6061-T6. Then I have 3 connections, one is a fixed point on the base plate that would attach to the shell worn by the user. The next two are bearing supports around the upper shaft to simulate the bearings that will be in place. Then for external loads I use a torque load of 120N*m within the casing where the motor would sit and a vertical force of the reactional load from the movement of the lower leg. This is equal to 441 N of force.

Results & Discussion

Starting off we have the calculations for the yield stresses for each of the designs. We do this by using equation 11, 12, and 14 for this calculation. As we plug everything in for the current design, we get a yield stress of $\sigma = 0.314$ MPa. Whereas for the new design we get a yield stress equal to $\sigma = 0.04356$ MPa. For our goal of a maximum yield for aluminum with a FOS of 2 we can see that both of these designs would work and not yield during these load paths. One observation is that the current design has over a 7x lower yield stress than the current design. When looking at this number and the decrease in cost and weight, I can make the decision that the new design will be a more effective and stronger design.

In addition, to this I looked at the side mounted brackets to determine if they would have a large enough factor of safety around the edges of the bearings. This is slightly similar to the last calculation using equations 11, 13, 14, and 15. I used the outer diameter of the top of the frame of 46.11mm and the diameter of the bearing of 40mm to solve for I and then used a Moment with the thickness of the plate to get a $\sigma = 42.55$ MPa. Then, plugging this into equation 15 you get a factor of safety of 3.24. This FOS is within the range of FOS we desire as it is greater than 2. However, there isn't much room for error and could possibly be a point of failure if something does not encounter in this calculation takes place. Despite this it does seem likely that it would be a usable design for this prosthetic leg frame, and it would be able to withstand the forces necessary.

With the FEA we can notice many things that help to prove the factor of safety is within the minimum 2 desired. The first interesting thing I noticed is the stress, and that it follows similarly to my calculations with little to know stress within the bearings of the frame. Another interesting thing is, the difference of the displacement of the designs. Both designs do have small variations, however it can be seen that the new design has a smaller displacement of 0.8668 compared to the 0.9920 seen within the current design. This analysis helps to demonstrate the differences and supports the switch from the current design to the new design. In conclusion through the use of yield stresses, FOS, and FEM Analysis, we now know that the New design is a better option than our current one and this will impact our project as we will be switching the lower part over to this newer design.

Battery Time Analysis – Aiden Camisa

This analysis outlines the electrical power and battery sizing requirements for an active hip prosthetic based on the desired time. Mathematical modeling using sinusoidal approximations for hip motion and torque interpolations helps to set requirements for the battery. These assumptions stated that were found from using the interpolations are based on a 90kg individual and 48 N*m continues torque with a possible peak torque of 120 N*m. In addition we assumed a baseline FOS of 2 and this is built into all of our calculations done throughout this analysis. Equations that were used and necessary are:

$$\theta(t) = \theta_0 + A \sin\left(\frac{2\pi t}{T}\right) \quad (16)$$

$$\omega(t) = \frac{d\theta}{dt} = A \cdot \frac{2\pi}{T} \cos\left(\frac{2\pi t}{T}\right) \quad (17)$$

$$E = \int_0^T \frac{\max(P_{mech}(t), 0)}{\eta_{motor}} dt + P \cdot T \quad (18)$$

Where $\theta(t)$ is the angle with respect to time, θ_0 is the initial angle, $\omega(t)$ is the angular velocity (rad/s), P_{mech} is the mechanical power (W), and E_{step} is the electrical energy per step. The results are in the table below:

Time (Min)	Battery required (Wh)
10	21.73
20	43.46
30	65.19
45	97.79
60	130.38
90	195.57

Table 1: Battery based on Time Requirement

Above in the table we can see results of the battery required in Watt Hours for each of these times. This does include a Factor of safety of 2 within these results. This information was beneficial as it initially brought up a additional conversation of what our desired time should be. From here we chose to aim for a more realistic time frame which meant for us looking at as long as possible. This allowed us to assist in narrowing down our desired battery.

Shaft Analysis – Victoria Lyon

Based on a kinematic study in which data is used in the motor analysis, the ranges of torque and moment applied to the hip joint can be used to analyze the shaft and axle present in the design. Note that the shaft and axle are both stepped, with keyways and notches for retaining rings. Therefore, it is necessary to analyze the potential failure that could occur due to these stress concentrations. The initial material selected is AISI 1050 CD steel, $S_{ut} = 690 \text{ MPa}$, $S_y = 580 \text{ MPa}$. The shaft and axle have identical diameters, both of which have $d_1 = 17 \text{ mm}$ on either side for bearing fitting, and $d_2 = 19.02 \text{ mm}$ in the center to secure the gears. There are no fillets on the shaft or axle due to manufacturing simplicity. The lower shaft additionally features a flange for attachment to the motor and is used to transmit the torque for hip rotation, in which we place the main focus of the analysis on.

Using the modified Goodman relation, the factor of safety is computed using the following equation:

$$n = \left(\frac{\sigma_a'}{S_e} + \frac{\sigma_m'}{S_{ut}} \right)^{-1} \quad (19)$$

The fluctuating von Mises stresses used above are calculated using the midrange and alternating torque and moment:

$$\sigma_a' = \left[\left(\frac{32K_f M_a}{\pi d^3} \right)^2 + 3 \left(\frac{16K_{fs} T_a}{\pi d^3} \right)^2 \right]^{1/2} \quad (20)$$

$$\sigma_m' = \left[\left(\frac{32K_f M_m}{\pi d^3} \right)^2 + 3 \left(\frac{16K_{fs} T_m}{\pi d^3} \right)^2 \right]^{1/2} \quad (21)$$

The resulting factor of safety is $n = 1.23$. The shaft meets maximum activity requirements but may require further optimization for increased security.

Key Design – Victoria Lyon

It is typical fashion to design a shaft key of a similar, yet weaker material that would fail first before other components. With this in mind, a steel of the same series as the shaft is initially selected, AISI 1040 CD steel which has a yield strength of:

$$S_{y_k} = 490 \text{ MPa}$$

To begin designing the rest of the key, first, the maximum permissible shear stress for the shaft is determined, in which the equation is written as:

$$\tau_s = \frac{S_y}{2 * n} \quad (19)$$

Where n is the factor of safety. For initial design, the factor of safety will be taken as $n = 1$. Therefore, the maximum permissible shear stress for the shaft is $\tau_s = 290 \text{ MPa}$. Next, the maximum permissible crushing stress for the key is computed, written as:

$$\sigma_c = \frac{S_y}{n} \quad (20)$$

In which the maximum crushing stress is equal to the material yield strength of $\sigma_c = 490 \text{ MPa}$. Similarly as computed for the shaft, the maximum permissible shear stress for the key is then determined:

$$\tau_k = \frac{S_y}{2 * n} \quad (21)$$

The maximum permissible shear stress the key is able to handle is calculated to be $\tau_k = 245 \text{ MPa}$. Lastly, based on the previously computed values, the maximum torque experienced is computed:

$$T = \frac{\pi}{16} * \tau_s * D^3 \quad (22)$$

Yielding a maximum torque of $T = 8.8 \times 10^5 \text{ N} * \text{mm}$. With each of these values, the length of the key can be determined based on analysis for both shear and crushing stresses, as written:

$$\tau_k = \frac{2T}{D * b * l} \quad (23)$$

$$\sigma_c = \frac{4T}{D * b * l} \quad (24)$$

Solving each equation for length, l , simultaneously yields a result of $l = 45.3 \text{ mm}$. The final key dimensions are as follows: $w = 6.35 \text{ mm}$, $h = 4.76 \text{ mm}$, and $l = 45.3 \text{ mm}$.

Bearing Selection – Victoria Lyon

Based upon typical human gait, the team previously computed that the leg experiences about 1324 N in ground-reaction forces, composed of 1244 N which is radial, and 453 N which is axial. Accounting for forces in both directions, an angular contact ball bearing will be selected.

In order to select a preliminary set of suitable bearings, we take into account the shaft diameter of $d = 17 \text{ mm}$. This measurement will be used as a bore size in catalogs, and applicable bearings will be selected and thus computed for factors of safety. To fit a $d = 17 \text{ mm}$, a Timken single row angular contact ball bearing 7203 B [1] is selected. This bearing has a dynamic load rating of $C_{10} = 9.93 \text{ kN}$ and static load rating of $C_0 = 5.54 \text{ kN}$, which is more than suffice for the current application forces. To determine the factor of safety, we take the static load rating divided by the ground force reaction:

$$n_{bearing} = \frac{C_0}{1324} \quad (25)$$

Resulting in a factor of safety of $n_{bearing} = 4.18$. 3 of these bearings will be used in the system, in which it remains highly secure that the selected bearing can handle the applied.

Torque Analysis for Hip Flexion – Matt Martinez

To estimate the torque required for hip flexion, the leg was modeled as a rigid body, restricted to the sagittal plane, and subjected to gravitational loading and joint geometry constraints. This calculation represents a scenario, where the hip joint must support the full weight of the body. The cases analyzed correspond to maximum hip flexion ($\theta = 90$) at three different knee flexion angles (0, 60, 90). These were selected to represent different postures and to produce different moments around the hip joint.

Equations and Solutions

Two equations were used to describe the static torque at the hip:

$$\tau = rF\sin\theta \quad (26)$$

Where τ is the joint torque (N·m), F is the applied muscle or actuator force (N), and r is the effective moment arm length (m). Using this relationship, the total static hip torque was modeled as the sum of moments generated by the thigh, shank, and foot segments:

$$\tau_{hip}(\theta, \beta) = m_{thigh}gr_{thigh}\sin\theta + m_{shank}g(L_1\sin\theta + r_{shank}\sin(\theta - \beta)) + m_{foot}g(L_1\sin\theta + L_2\sin(\theta - \beta)) \quad (27)$$

Where m is the mass (kg), g is gravitational acceleration (9.81 m/s^2), L is the length (m), θ is the hip flexion angle ($^\circ$), β is the knee flexion angle ($^\circ$), and r is the center of mass (m). MATLAB was used to evaluate Equation () across a continuous range of knee flexion angles and to generate the resulting torque curve:

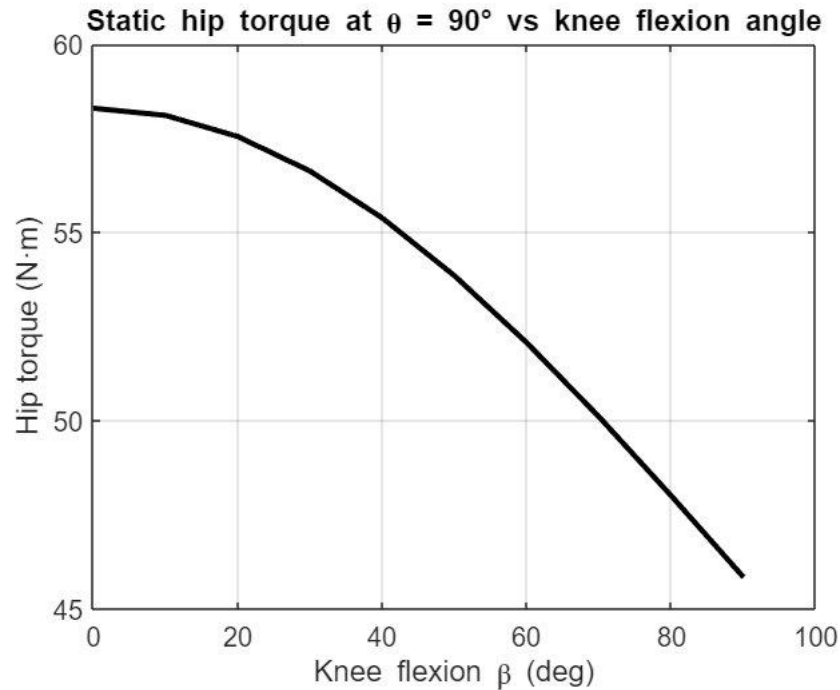


Figure 14: Static Hip Torque vs. Knee Flexion Angle

The plot shows that static hip torque decreases from 58.3 N·m at 0° knee flexion to 45.8 N·m at 90°. The results show that the maximum hip torque demand occurs when the knee is fully extended and gives an idea of a maximum torque that the hip would experience.

Design Implications

This analysis gave us a rough estimation of the minimum constant torque requirement of 58.3 Nm for the hip actuator under static conditions. However, this information would end up not being very useful as the team was given more accurate hip joint data sets, during various activities, which would be modeled in MATLAB and directly compared with various motors.

Joint & Motor Analysis – Matt Martinez

The joint and motor analysis models human hip motion during normal gait, to select appropriate motors and gearing. Unlike the previous analysis analyzing static torque, this analysis used time-varying biomechanical data for hip kinematics over a full gait cycle (1.2 s). These conditions provide better estimations of motor sizing and power. The torque of the hip is given and then factored by body weight (BW). The motor chosen is only used as a benchmark to illustrate the analysis.

Equations and Solutions

$$\tau_{hip} = -BW \cdot \tau \quad (28)$$

Other variables calculated for the hip joint are angular velocity (ω_{hip}) in rad/s and power (P_{hip}) in watts. θ is the hip angle in degrees.

$$\omega_{hip} = \frac{d\theta}{dt} \quad (29)$$

$$P_{hip} = \tau_{hip} \cdot \omega_{hip} \quad (30)$$

Results were calculated and then modeled using MATLAB. Below are the kinematics at the hip joint during normal gait over one cycle:

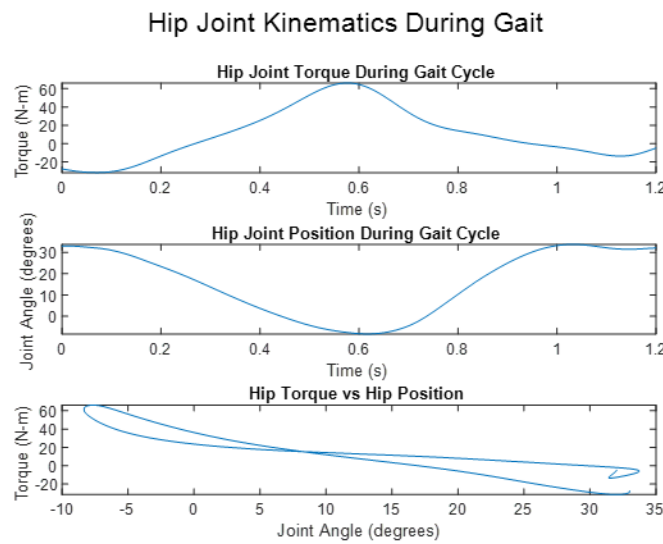


Figure 15: Hip Joint Kinematics During Gait Cycle

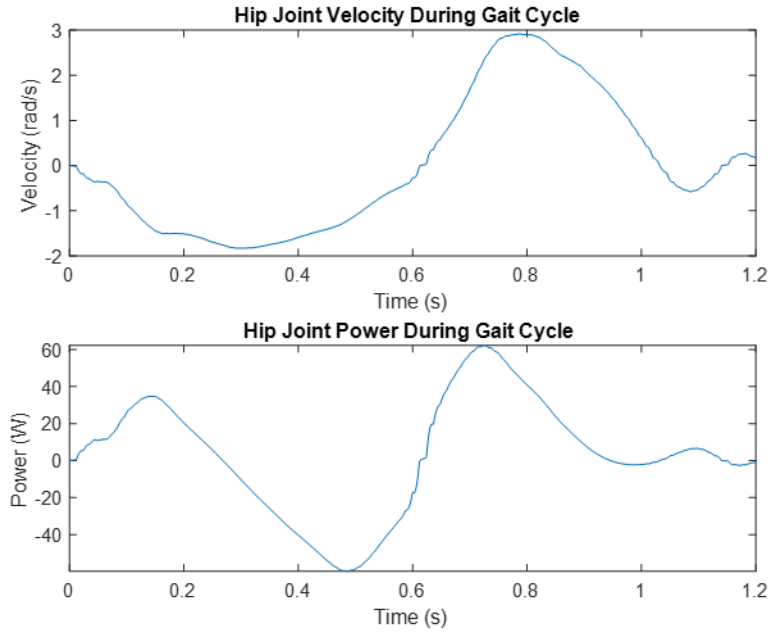


Figure 16: Hip Joint Velocity and Power During Gait Cycle

Next, the specifications from the chosen motor are used to find the current (I) in amps, voltage (V) in volts, and power (P) in watts.

$$I = \frac{\tau_m}{k_t} \quad (31)$$

$$V = IR + k_t \omega_m \quad (32)$$

$$P = V \cdot I \quad (33)$$

τ_m is motor torque (Nm), k_t is the torque constant (Nm/A), R is resistance (Ω), and ω_m is the motor angular velocity (rad/s). The following graphs show these models:

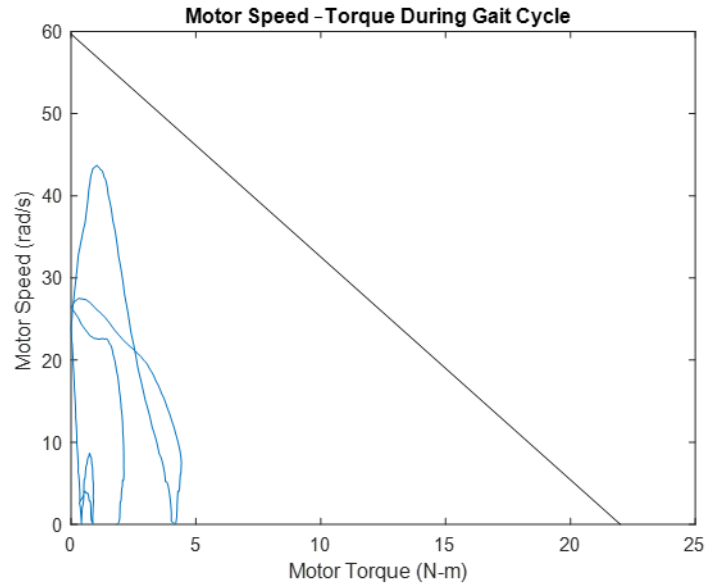


Figure 17: Motor Speed-Torque During Gait

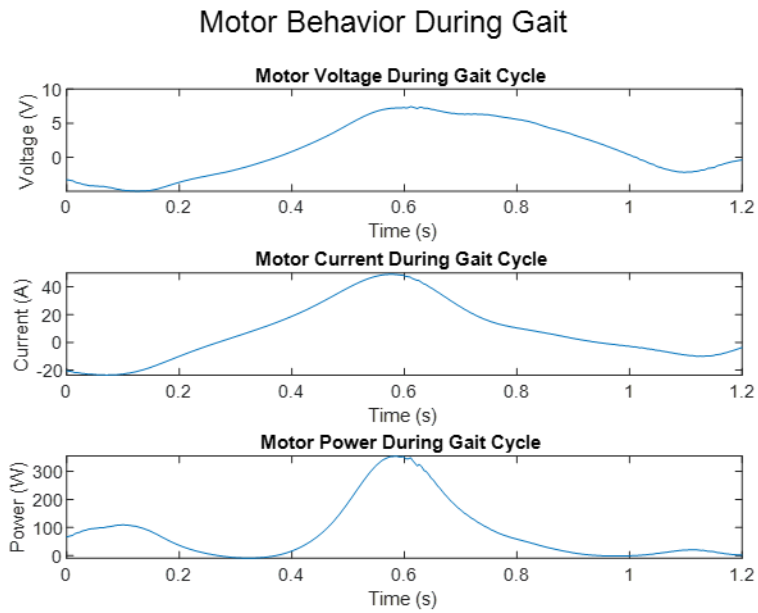


Figure 18: Motor Behavior During Gait

Design Implications

The AK80-9 motor used was found to meet torque and power needs, but high gear ratios increased inefficiency. This analysis was extremely useful as it used realistic torque, speed, and power demands during walking. It allowed the team to plug in other various motors, and their specifications in order to find the optimal choice to power the hip prosthesis with a maximum torque output and minimal gear ratio.

Gear Design Analysis – Matt Martinez

The purpose of this analysis was to select an optimal gearset for the powered hip prosthesis capable of transmitting the required torque during normal gait. This analysis used torque, velocity, and power demands from the MATLAB models using the CubeMars AK60-84 KV80 (chosen motor). The maximum operating requirements for the gearset are: 585.9 lb-in of maximum torque, 0.084 hp of maximum power, and 27.7 of maximum speed. To account for operating conditions aligning with mostly uniform shock via Boston Gears, a service factor of 1.25 was applied. This resulted in a required transmitted torque of 732.4 lb-in.

Equations and Solutions

Allowable torque (T) and horsepower (HP) per RPM per gear design are listed in Boston Gears' catalog and are accurate. Equations used to calculate these, as well as allowable load (W), are also listed and shown below:

$$W = \frac{SFY}{P} \left(\frac{600}{600+V} \right) \quad (34)$$

$$T = \frac{W \times D}{2} \quad (35)$$

$$HP = \frac{WV}{33000} \quad (36)$$

SF is the safety factor, Y is tooth form factor, P is diametral pitch, V is pitch line velocity, and D is diameter. Equation 1 is for a spur gear. To calculate allowable load of a helical gear, diametral pitch is replaced with normal diametral pitch. Tooth form factors are based on number of teeth and are shown in the tables below:

Number of Teeth	14-1/2° Full Depth Involute	20° Full Depth Involute
10	0.176	0.201
11	0.192	0.226
12	0.210	0.245
13	0.223	0.264
14	0.236	0.276
15	0.245	0.289
16	0.255	0.295
17	0.264	0.302
18	0.270	0.308
19	0.277	0.314
20	0.283	0.320
22	0.292	0.330
24	0.302	0.337
26	0.308	0.344
28	0.314	0.352
30	0.318	0.358
32	0.322	0.364
34	0.325	0.370
36	0.329	0.377
38	0.332	0.383
40	0.336	0.389
45	0.340	0.399
50	0.346	0.408
55	0.352	0.415
60	0.355	0.421
65	0.358	0.425
70	0.360	0.429
75	0.361	0.433
80	0.363	0.436
90	0.366	0.442
100	0.368	0.446
150	0.375	0.458
200	0.378	0.463
300	0.382	0.471
Rack	0.390	0.484

Table 2: Y Factor for Spur Gears

FOR 14-1/2°PA-45° HELIX ANGLE GEAR			
No. of Teeth	Factor Y	No. of Teeth	Factor Y
8	.295	25	.361
9	.305	30	.364
10	.314	32	.365
12	.327	36	.367
15	.339	40	.370
16	.342	48	.372
18	.345	50	.373
20	.352	60	.374
24	.358	72	.377

Table 3: Y Factor for Helical Gears

The gearsets below show the first for each gear type and diametral pitch that can sustain the required load. They were pulled from the Boston Gears catalog [2]. Each table lists the gear teeth, allowable power, allowable torque, diametral pitch, face width, and diameter. These were used to calculate the volume of the gear, which was then compared to the torque to find which gear produces the most torque per unit volume. This is what was used to choose the right gear as space minimization and torque maximization is important.

Each gear is also made of hardened steel. This is because during the analysis, it was noticed that hardened steel is much stronger than bronze, and much lighter than cast iron, making it the perfect medium material.

Teeth	Power (HP)	Torque (lb-in)	P (Teeth/in)	Face Width (in)	Diameter (in)	Volume (in ³)	Torque per Unit Volume (T/V)
25	.29	742	10	1	2.5	4.91	151.12
11	.38	946	6	1.5	1.83	3.95	239.49
16	.31	778	8	1.25	2	3.93	197.96

Table 4: Spur Gear Specifications with Pressure Angle of 14.5

Teeth	Power (HP)	Torque (lb-in)	P (Teeth/in)	Face Width (in)	Diameter (in)	Volume (in ³)	Torque per Unit Volume (T/V)
64	.31	779	16	.75	4	9.42	82.7
36	.37	928	12	1	3	7.07	131.26
20	.31	784	10	1.25	2	3.93	199.49
14	.35	890	8	1.5	1.75	3.61	246.54

Table 5: Spur Gear Specifications with Pressure Angle of 20

Teeth	Power (HP)	Torque (lb-in)	P – Normal P (Teeth/in)	Face Width (in)	Diameter (in)	Volume (in ³)	Torque per Unit Volume (T/V)
30	.32	818	10 – 14.14	.875	3	6.19	132.15
24	.34	862	8 – 11.31	.75	3	5.3	162.64
16	.29	740	8 – 11.31	1	2	3.14	235.67
10	.3	758	6 – 8.48	1	1.67	2.19	346.12
10	.38	948	6 – 8.48	1.25	1.67	2.74	345.99

Table 6: Helical Gear Specifications with Pressure Angle of 14.5

Based on the analysis, both helical gears with 10 teeth in Table 7 are the most ideal as they have the highest torque per unit volume. For an extra buffer, it would be best to go with the option with a higher face width, which increases the torque. This means the gearset's max allowable torque will be 948 lb-in. The choice is also perfect as the bore size matches the team's assumption of .75 in.

Going back to the gear catalog, the gears are found (right-hand/left-hand) along with their catalog numbers and Item Codes. There is also information about a keyway, which will most likely be needed to fasten the gears on the shafts.

6 TRANSVERSE DIAMETRAL PITCH						Face without Hubs = 1.250" -with Hubs = 1.000" Overall Length = Face + Hub Proj.					
STEEL-HARDENED											
8	1.333	.625	-	-	1/8 x 1/16		H608R	18000	H608L	18002	
10	1.667	.750	-	-	3/16 x 3/32		H610R	18004	H610L	18006	
12	2.000	1.000	-	-	1/4 x 1/8	A	H612R	18010	H612L	18008	
15	2.500						H615R	18014	H615L	18012	
18	3.000						H618R	18018	H618L	18016	
24	4.000						H624R	18022	H624L	18020	
8	1.333	.625	1.00	.75	1/8 x 1/16	A	HS608R	18024	HS608L	18026	
9	1.500	.750	1.18	.75	3/16 x 3/32		HS609R	18028	HS609L	18030	
10	1.667		1.34	.75			HS610R	18032	HS610L	18034	
12	2.000	1.000	1.62	.75	1/4 x 1/8		HS612R	18036	HS612L	18038	
15	2.500	1.250	2.00	.75	5/16 x 5/32		HS615R	18040	HS615L	18042	
18	3.000		2.25			HS618R	18044	HS618L	18046		
20	3.333		2.50			.75	5/16 x 5/32	HS620R	18048	HS620L	18050
24	4.000							HS624R	18052	HS624L	18054
30	5.000							HS630R	18056	HS630L	18058
36	6.000							HS636R	18060	HS636L	18062

Table 7: Helical Gear Catalog with Chosen Gear Highlighted.

The final gear choice was the helical gears with 10 teeth, 1.667 in diameters, .75 bore sizes, and 1.25 in face widths. The catalog numbers and item codes are H610R – 18004 (right-hand) and H610L – 18006 (left-hand).

Design Implications

This analysis was necessary in order to ensure that there were no mistakes when purchasing a big part of the mechanical component budget. The gears selected were then intended to be 3D printed and used for the team's Prototype 2. They were thought to be sufficient, but an extra assumption was missed during the analysis: the diametral pitch must have been three inches so that the gears could properly mesh with each other. This was then quickly solved and new gears were chosen that had a more than sufficient FoS.

Factors of Safety

Sub-system	Part	Load Case Scenario	Material	Method of Computing FoS	Minimum FoS
Mechanical					1
	Frame	Maximum torque, maximum user force, and moment force	Aluminum 6061-T6	FEA	3.24
	Shaft	Maximum torque and moment in gait cycle	AISI 1050 CD steel	MATLAB script	1.23
	Key	Maximum torque and moment in gait cycle	AISI 1040 CD	Manual	1
	Bearing	Maximum ground-force reaction on hip	Polyamide cage, high-carbon chrome steel balls	Manual	4.18
	Gears	Gait cycle with moderate shock	Hardened Steel	Catalog Service Factor	≥ 1.25
Electrical					1.8
	Battery	Loaded for a 24V motor	Lithium	Manual	1.8
	Motor	Loaded with 22Nm of torque	Many, Steel holds the shafts	Not Applicable	N/A

Table 8: FOS Table

Flow Charts & Diagrams

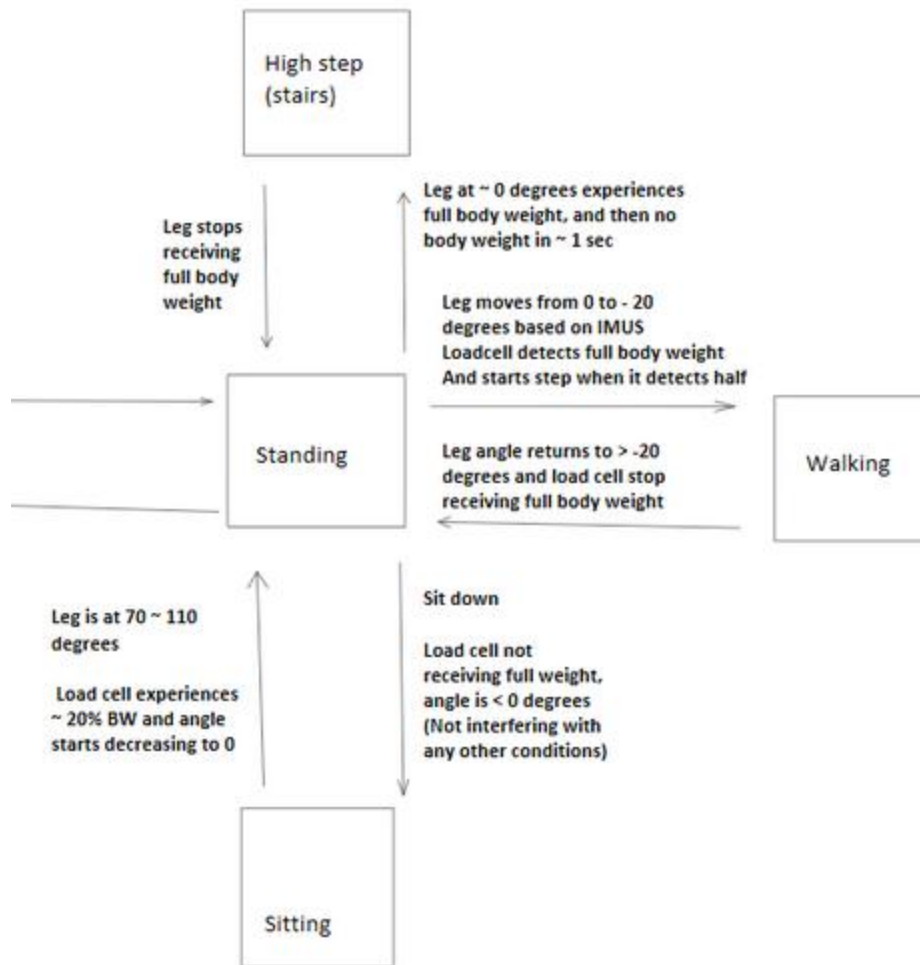


Figure 19: Control Plan Flow Chart

The above flow chart is the Teams plan for implementing a control code into our motor control system. The code details specific conditions for the leg such as sitting or walking and then details the requirements for the motor to activate and turn the leg into that condition.

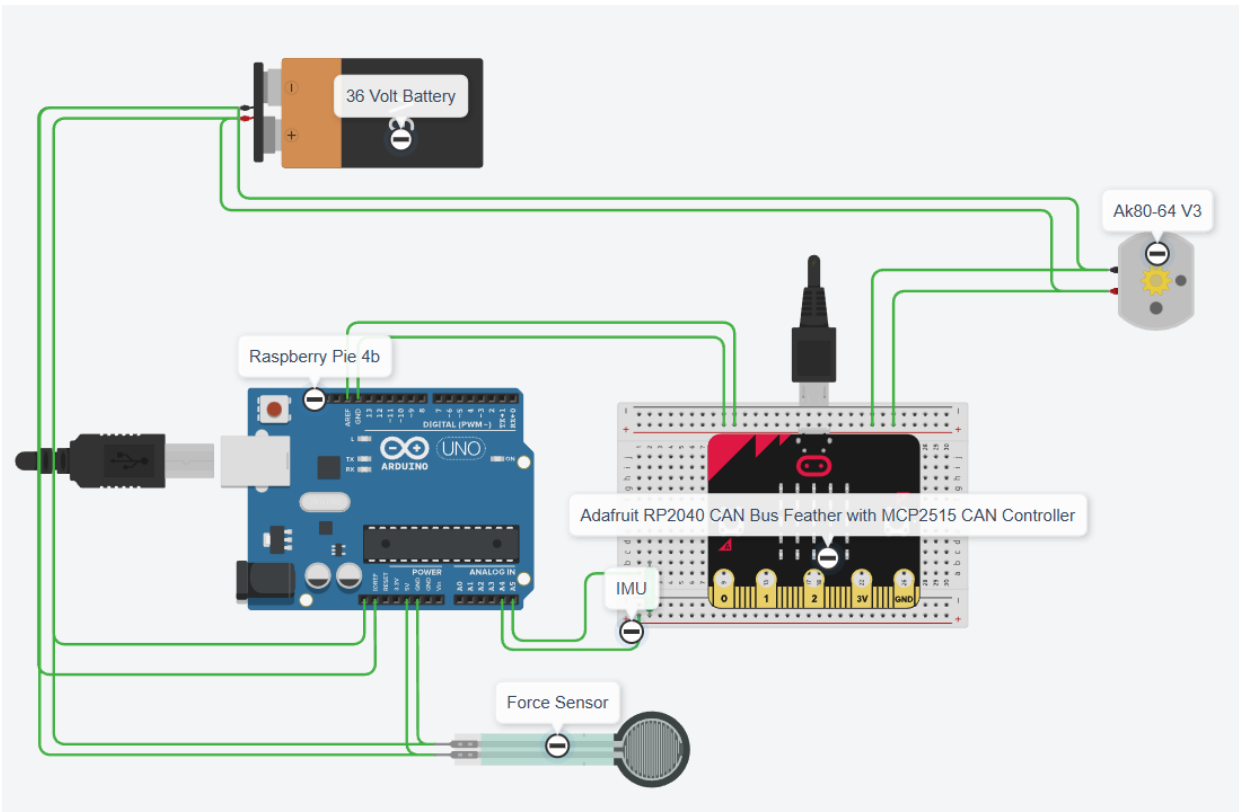


Figure 20: Circuit Diagram for Control Methods

Above is the image of the circuit diagram using the software TinkerCAD. Here we can see the system using a IMU and a Force Sensor as input into the raspberry pie 4b then this information travels through to a Adafruit RP2040 CAN bus which converts the message into CAN communication which is then given to the motor. This is all powered by our 36V battery which has additional buck converters which are not represented in this image. There were some limitations to the understanding and abilities of TinkerCAD and what systems it has available, such as the specific parts including Raspberry Pi's and buck converters.

Moving Forward

Through this document, it can be seen that many of our analysis that have been carried out have been useful within our final design. Many of our initial calculations were done to determine some factors that would help narrow down our search for specific items. This included things like our battery and motor sections. As we have gotten further into our project, the analyses have switched more to confirming what our design is and making sure that our factor of safety is up to our standards. While many of these parts have had an initial analysis done, the need for new and updated analyses has also come up.

Analyses to Rework

In addressing current completed analyses, the need for new and updated analyses has also come up. Items such as the shaft and key require updating in failure analysis and layout designs. Per client and professor recommendations, the lower shaft and upper axle need a corrected geometry for retaining rings (square notches rather than circular), removal of shoulder file for manufacturing simplification, and

therefore material analysis to ensure that with no filets for stress-propagation, the shaft and axle will handle the activity and load necessary. Proper analysis with a keyway also must be done, as the additional incision to the shaft creates more stress concentration. The upper axle must also consider the loading and shear from socket-connection and must be able to handle the bending and shear that will be applied at this location. The key is to be designed shorter, for improved shear stress management and analyzed for failure and updated factor of safety.

Analyses to be Done

An analysis for a connection plate must also be done—this plate is what the entire hip joint and prosthetic leg are to be mounted to and must have a geometry that adequately distributes stresses and securely holds the prosthetic in place. In addition to these items there are some additional calculations and wiring that need to be finalized for the electrical system of our project. This mostly comes in the form of implementing the battery and the sensors to the overall system. There has been progress in getting the system to run using a stand in power source, however we will need to have additional calculations within this system to make sure our device is safe and will not fail.

References

[1] The Timken Company, *Timken® Angular Contact Ball Bearing Catalog*, Order No. 11193, The Timken Company, PDF, 2019. Available: https://www.timken.com/resources/timken-angular-contact-ball-bearing-catalog_11193/

[2] Boston Gear, *Boston Gear Product Catalog P-1930-BG*. Quincy, MA: Boston Gear, 2019. Accessed: Nov. 22, 2025.

Appendix

A: Shaft Analysis MATLAB Script

```
% Victoria Lyon
% ME 486C Spring 2026
% Shaft Fatigue Failure & FoS Analysis

% AISI 1050 CD (Pa)
Sut = 690e6;
Sy = 580e6;
Se_prime = 345e6;

% Smallest diameter, m
d = 0.017;

% Loads (Nm)
Ma = abs(-38.5);
Mm = abs(-8.5);
Ta = abs(40);
Tm = abs(20);

% Endurance Limit & Factors
ka = 0.9065; % Ground finish
kb = 0.9157; % Size factor
kc = 1; % Load factor
kd = 1; % Temp factor
ke = 0.753; % 99.9% reliability

Se = ka*kb*kc*kd*ke*Se_prime;

% Stress concentration for stepped shaft w/ no radii
Kf = 1.6;
```

```
Kfs = 1.3;

% Stresses
sigma_a = sqrt( ...
    ((32*Kf*Ma)/(pi*d^3))^2 + ...
    3*((16*Kfs*Ta)/(pi*d^3))^2 );

sigma_m = sqrt( ...
    ((32*Kf*Mm)/(pi*d^3))^2 + ...
    3*((16*Kfs*Tm)/(pi*d^3))^2 );

% Modified Goodman FoS
n = 1 / ((sigma_a/Se) + (sigma_m/Sut))
```